Available online at www.sciencedirect.com
SCIENCE DIRECT®

ELSEVIER

Journal of Sound and Vibration 274 (2004) 1065–1078

JOURNAL OF SOUND AND VIBRATION

www.elsevier.com/locate/jsvi

Letter to the Editor

Experimental evaluation of augmented UD identification based vibration control of smart structures

Chengli He, Ratneshwar Jha*

Department of Mechanical and Aeronautical Engineering, Clarkson University, P.O. Box 5725, CAMP Building, Potsdam, NY 13699-5725, USA

Received 10 January 2003; accepted 8 September 2003

1. Introduction

The technology of smart materials and structures represents an emerging multidisciplinary field of study with applications ranging from mechatronic structures to automobiles and spacecraft [1]. Smart material based actuators and sensors are integrated with a host structure to enhance system performance through reduced vibrations, active shape control, accurate pointing, etc. The practical application of smart structures is increasing because of the commercial availability of smart materials based actuators/sensors and developments in related technologies. The real time sensing and actuation capabilities of smart structures provide a powerful means for active vibration control. Active vibration control makes it possible to achieve unequalled performances in areas where passive methods have shown their limits. Vibration reduction is essential for high-precision machining, high accuracy inspection, human comfort, acoustics, and extended lifetime. Piezoelectric materials have been used extensively as actuators and sensors in smart systems, usually bonded to the surfaces of the structures.

The control algorithm forms a vital part of a smart structure. It analyzes sensor inputs and commands the actuators to respond to the external (or internal) excitation in real time. The conventional control systems using classical or state space techniques require a high fidelity model of the plant (smart structure). The plant models, generally based on finite element analysis or experimental identification, are very difficult to obtain for complex structures. The complex smart structures, such as deployable space telescope and morphing aircraft, need to employ a large number of distributed sensors and actuators. Such systems are likely to exhibit non-linearity and variations with time. Adaptive control systems are suitable for the challenges presented by these complex systems. The basic idea in adaptive control is to estimate the plant parameters based on the measured signals and calculate the control input using the estimation [2]. Adaptive control can maintain consistent performance of a system in the presence of uncertainty or unknown variation

*Corresponding author. Tel.: +1-315-268-6438; fax: +1-315-268-7686.
E-mail address: ratan@clarkson.edu (R. Jha).

0022-460X/$ - see front matter
doi:10.1016/j.jsv.2003.09.027

in plant parameters. Another advantage of adaptive control is that it requires limited *a priori* knowledge of the plant to be controlled. A recent review of the various adaptive control techniques is presented in Ref. [3].

Generalized predictive control (GPC) [4,5] provides a robust algorithm for challenging adaptive control applications. The GPC algorithm uses a receding-horizon strategy to predict plant output over several steps based on assumed future control inputs. It is known to control non-minimum phase plants, open loop unstable plants and plants with variable or unknown dead time. It is also robust with respect to modelling errors, over and under parameterization, and sensor noise. It has been proved to be efficient, flexible, and successful in many applications. Recently, an evaluation of modern adaptive multi-input multi-output (MIMO) control techniques for active stability augmentation and vibration control of tiltrotor aircraft showed GPC based MIMO active control to be highly effective [6].

The adaptive generalized predictive control (AGPC) technique, which combines the advantages of GPC and the adaptive plant model identification, is the subject of the present work. The corner stone of this algorithm is the predictive plant model whose parameters are estimated from online measurements. The parameter estimation method needs to be efficient for real time vibration control of smart structures. Most of the researchers use a conventional recursive least squares (RLS) [2] method to identify the plant model online. However, the conventional RLS algorithm has a number of shortcomings, such as poor robustness especially when implemented on computers with finite precision [7]. Also, the RLS algorithm is known to have optimal properties when the parameters are time invariant, but it is unsuitable for tracking time-varying parameters [8]. In order to improve the estimation method, Bierman [9] proposed UD factorization algorithm, which has a much better numerical performance than RLS. However, the UD factorization algorithm has not been as widely used as RLS because it appears to be more complicated to interpret and implement.

Niu et al. [7] proposed an augmented UD identification (AUDI) algorithm by rearranging the data vectors and augmenting the covariance matrix of Bierman's UD factorization algorithm. The AUDI permits simultaneous and recursive identification of the model parameters plus the loss function for all orders from 1 to n at each time step with approximately the same calculation effort as the nth order RLS and it has better numerical properties. The AUDI approach provides many features that are particularly suitable for real time applications. It provides other information in addition to the model parameters, such as model order and loss functions, parameter identifiability, noise variance, and signal-to-noise ratio.

The AUDI method has been implemented by some researchers. Clarke [10] developed an adaptive predictive control algorithm using the AUDI identification method (instead of RLS) and showed its effectiveness through simulations. Maniar et al. [11] evaluated the performance of the MIMO AGPC algorithm based on AUDI (with and without constraints) by experimental application on a computer-interfaced, pilot-scale process. However, no work has been reported using AUDI based adaptive predictive control of smart structures. Unlike most of the process control applications, smart structures have fast dynamics and, therefore, need efficient real time application algorithms. The current effort is to implement this algorithm in real time and investigate the experimental performance of the AUDI based AGPC in the vibration suppression of smart structures.

2. Adaptive generalized predictive control

The AGPC system can be described by the diagram as shown in Fig. 1. There are mainly four parts in this system: the plant to be controlled, adaptive plant model identification (which is used to adaptively predict the output of the plant), the desired plant output, and the performance index optimization process. The AGPC algorithm operates in two modes, namely, adaptive prediction and control. The adaptive prediction occurs between samples and the performance index optimization algorithm minimizes a user specified performance index to calculate the next control vector by using the predicted future output from the plant model.

2.1. Plant model description

Most single-input single-output plants, when considering operation around a particular set-point and after linearization, can be described by the controlled auto-regressive moving average model (CARMA). To model the non-stationary disturbance, such as random steps occurring at random times and Brownian motion, the controlled auto-regressive integrated moving average (CARIMA) model is more appropriate, which is given by [4]

$$A(z^{-1})y(k) = B(z^{-1})u(k-1) + \frac{\xi(k)}{\Delta}, \tag{1}$$

where $y(k)$ is the predicted plant output at time step k, $u(k-1)$ is the plant input at the time step $k-1$, $\xi(k)$ is an uncorrelated random sequence, Δ is the differencing operator $1-z^{-1}$, and the $A(z^{-1})$, $B(z^{-1})$ are the polynomials in the backward shift operator z^{-1} as follows:

$$A(z^{-1}) = 1 + a_1 z^{-1} + \cdots + a_{n_a} z^{-n_a}, \quad B(z^{-1}) = b_0 + b_1 z^{-1} + \cdots + b_{n_b} z^{-n_b}. \tag{2, 3}$$

If we use the filtered signals from the plant input–output data

$$y_f(k) = \Delta y(k), \quad u_f(k-1) = \Delta u(k-1), \tag{4, 5}$$

the plant model becomes

$$A(z^{-1})y_f(k) = B(z^{-1})u_f(k-1) + \xi(k) \tag{6}$$

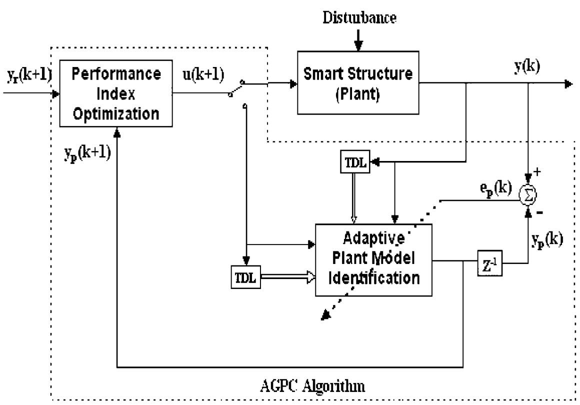

Fig. 1. Adaptive generalized predictive control (AGPC) system.

or

$$\begin{aligned} & y_f(k) + a_1 y_f(k-1) + \cdots + a_{n_a} y_f(k-n_a) \\ & \quad = b_1 u_f(k-1) + \cdots + b_{n_b} u_f(k-n_b) + \xi(k). \end{aligned} \tag{7}$$

To simplify notation, $y(k)$, $u(k)$ are used instead of $y_f(k)$, $u_f(k)$ for the rest of this paper, and $\hat{y}(k)$ is used to denote prediction. Thus, the resulting overall plant model with one-step-ahead prediction is given by

$$\begin{aligned} & \hat{y}(k) + a_1 y(k-1) + \cdots + a_{n_a} y(k-n_a) \\ & \quad = b_1 u(k-1) + \cdots + b_{n_b} u(k-n_b) + \xi(k). \end{aligned} \tag{8}$$

Defining the parameter and data (regressor) vectors as

$$\theta = [a_1, a_2, \ldots, a_n, b_1, b_2, \ldots, b_n]^{\mathrm{T}}, \tag{9}$$

$$h(k) = [-y(k-1), -y(k-2), \ldots, -y(k-n), u(k-1), u(k-2), \ldots, u(k-n)]^{\mathrm{T}}, \tag{10}$$

the above model can be rewritten as

$$\hat{y}(k) = h^{\mathrm{T}}(k)\theta + \xi(k). \tag{11}$$

An estimate $\hat{\theta}(k)$ of the true model parameter vector θ is obtained recursively at each sampling interval to predict plant response. The RLS algorithm [2] involves updating the covariance matrix in a way that can cause poor numerical robustness. Factorization of the covariance matrix into $\mathbf{UDU}^{\mathrm{T}}$ form, where $\mathbf{U}$ and $\mathbf{D}$ are a unit-upper-triangular matrix and a diagonal matrix respectively, and then updating $\mathbf{U}$ and $\mathbf{D}$ matrices (instead of the covariance matrix) improves the numerical performance [9].

2.2. Augmented UD identification

The AUDI method developed by Niu et al. [7,12] combines many nice properties and useful features into a single, compact, and flexible algorithm and provides a natural choice for control-oriented identification. Compared with the conventional RLS method, AUDI is simple in concept, robust in numerical performance, and versatile in application. The basic idea of AUDI is described briefly here.

With the one-step-ahead plant model described in the previous section and assuming the maximum order of the model is n and letting $n_a = n_b = n$, an augmented data vector is defined as

$$\begin{aligned} \boldsymbol{\Phi}_n(k) & = [-y(k-n), u(k-n), \ldots, -y(k-1), u(k-1), -y(k)]^{\mathrm{T}} \\ & = [\mathbf{h}_n^{\mathrm{T}}(k) - y(k)]^{\mathrm{T}}. \end{aligned} \tag{12}$$

The parameter vector is also rearranged in an analogous manner:

$$\hat{\boldsymbol{\theta}}_n(k) = [a_n, b_n, \ldots, a_2, b_2, a_1, b_1]^{\mathrm{T}}. \tag{13}$$

A new covariance matrix, called augmented information matrix (AIM) is defined as

$$\mathbf{A}_n(k) = \left[\sum_{j=1}^{k} \gamma^{k-j} \boldsymbol{\Phi}_n(j) \boldsymbol{\Phi}_n^{\mathrm{T}}(j) \right]^{-1}, \tag{14}$$

where γ is a forgetting factor. Decomposing $\mathbf{A}_n(k)$ into the $\mathbf{UDU}^{\mathrm{T}}$ form gives

$$\mathbf{A}_n(k) = \mathbf{U}_n(k)\mathbf{D}_n(k)\mathbf{U}_n^{\mathrm{T}}(k). \tag{15}$$

The above $\mathbf{U}_n(k)$ and $\mathbf{D}_n(k)$ matrices contain the parameter estimates and the loss functions for all model orders from 1 to n [7]. The AUDI permits simultaneous and recursive identification of the model parameters plus the loss function for all orders from 1 to n at each time step with approximately the same calculation effort as nth order RLS. The augmented **UD** identification approach provides many features that are particularly suitable for real time applications. There is no need to use RLS algorithm after UD factorization as required by Bierman's method [9].

2.3. Performance index

The GPC methodology minimizes a weighted sum of quadratic functions representing the predicted future errors and the control signal increments [4]:

$$J(N_1, N_2, N_u, \lambda) = \sum_{j=N_1}^{N_2} (y_r(k+j) - \hat{y}(k+j))^2 + \sum_{j=1}^{N_u} \lambda\, \Delta u^2(k+j-1). \tag{16}$$

The term $y_r(k+j)$ is the desired system output, $\hat{y}(k+j)$ is the predicted system output, $\Delta u(k+j-1)$ is the control increment, N_1 is the minimum costing horizon, N_2 is the maximum costing horizon, N_u is the control horizon, and λ is a control-weighting factor. The GPC approach uses a receding horizon strategy. At each time step k, the vector $\tilde{\mathbf{u}}$ comprising $\{\Delta u(k), \Delta u(k+1), \ldots, \Delta u(k+N_u-1)\}$ is calculated by minimizing the performance index J for the selected values of the parameters $\{N_1, N_2, N_u, \lambda\}$. The first element of vector $\tilde{\mathbf{u}}$ is used and $u(k) = u(k-1) + \Delta u(k)$ is sent as the control signal to the plant. The choice of the parameters in the performance index has a large impact on the performance of the control system. The term N_1 is set to its usual value of 1 (with no loss of stability if the dead time of the plant is not exactly known). The maximum costing horizon N_2 is also selected to be 1 since the plant model provides one-step-ahead prediction at each sample time. Multiple step-ahead prediction would require much larger computational expense for the plant with fast dynamics. The control horizon is an important design parameter since control increments are assumed to be zero after an interval N_u, that is, $\Delta u(k+j-1) = 0$ for $j > N_u$. The value of $N_u = 1$ is selected, which gives generally acceptable control for open-loop stable plants.

2.4. Optimal control law

With the one-step-ahead plant model and the horizons equal to 1 (as discussed above), the performance index can be rewritten as

$$J = [y_r(k+1) - \hat{y}(k+1)]^2 + \lambda[u(k) - u(k-1)]^2. \tag{17}$$

The minimization of the performance index gives the optimal control law as

$$u(k)_{optimal} = u(k-1) - \frac{\hat{y}(k+1)}{\lambda}\frac{\partial \hat{y}(k+1)}{\partial u(k)} = u(k-1) - \frac{\hat{y}(k+1)}{\lambda} b_1, \quad (18)$$

where the reference value (or desired system output) $y_r(k+1)$ is taken as zero for the task of vibration suppression. Since the system identification is done online with the presence of disturbances acting on the system, an estimated disturbance model is reflected in the identified system model and there is no need to model the disturbances separately [13]. The control algorithm was implemented by writing a C-file S-function used in MATLAB/Simulink.

3. Experimental evaluation

3.1. Experimental set-up

The experimental set-up (Fig. 2) comprises a thin plate clamped rigidly at the base, which is free to move up and down on linear bearings. An Electrodyne electromagnetic shaker (model AV-400) generates the excitation input for the structure. The shaker is powered by Electrodyne model N-300 single channel amplifier with a frequency range of 1.5 Hz to 22 kHz. Two ACX PZT actuators (QP10W) are bonded to the surface of the plate at the root, which is considered the best location for controlling the fundamental bending mode [14]. The actuator input is limited to ±100 V, which is well within the range of the maximum permissible voltage. Two Kistler piezoceramic shear accelerometers (model 8774A50) are connected to a Kistler signal conditioner that sends vibration information through a low-pass filter to the PC through AD channel. The frequency range for the PZT actuators and the accelerometers are 0–20 and 1–10 kHz, respectively. A 600 MHz PC is used for the data acquisition, analysis and control. The signals are converted from analog-to-digital and digital-to-analog using a Quanser 16-channel 12-bit AD/DA board. Only the tip accelerometer is used in the current research and both actuators receive the same voltage. Thus, we have a SISO (single-input single-output) control system. Fig. 3 shows the schematic diagram of the experimental set-up.

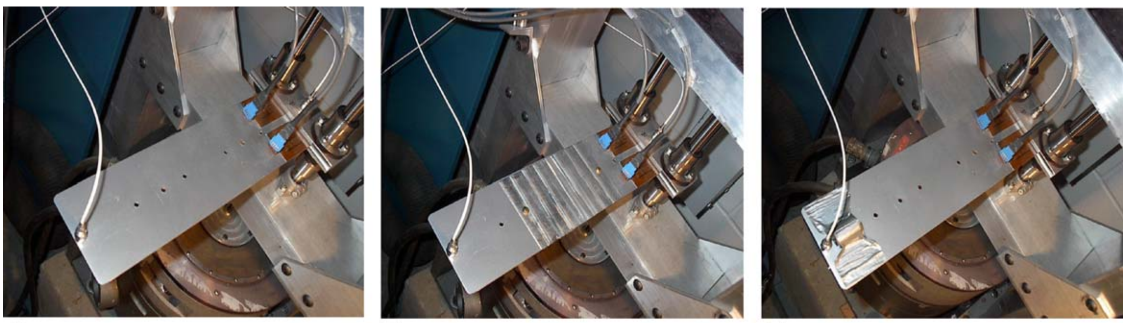

(a) (b) (c)

Fig. 2. Experimental set-up (a) original structure, (b) plate added and (c) tip mass added.

3.2. Experimental results and discussions

The AGPC system is applied to the vibration suppression of a smart structure as described in the previous section. The structure was excited by an impulse (generated through the shaker) and the tip acceleration was measured to obtain the natural frequencies. Fig. 4 shows the natural frequencies of the structure. The first two natural frequencies are 6.67 and 40.4 Hz for the original structure, 6.68 and 42.6 Hz for the plate-added structure, 5.33 and 38.5 Hz for the tip mass added structure. These two modes are cantilever (bending) modes. The magnitude of the tip acceleration is reduced due to the modifications, especially for the second mode with plate added which stiffens the middle part of the structure as shown in Fig. 2(b). To assess the performance of the control system, excitations at the first two natural frequencies and band-limited white noise (covering the first two modes) were subsequently used. The parameter vector of the CARIMA plant model was obtained in real time at the sampling frequency of 1000 Hz starting from random small initial

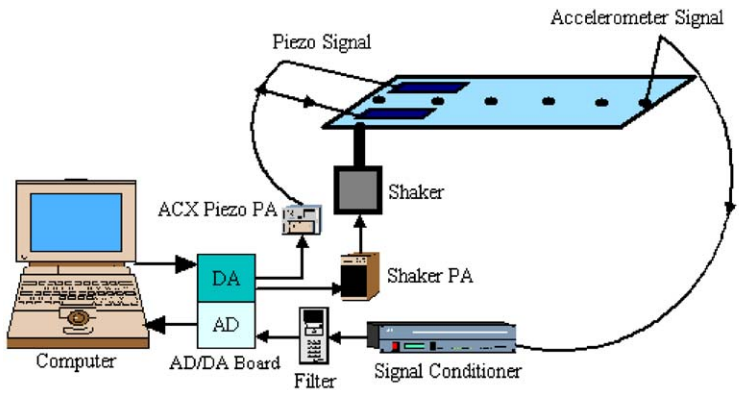

Fig. 3. Schematic diagram of the experimental set-up.

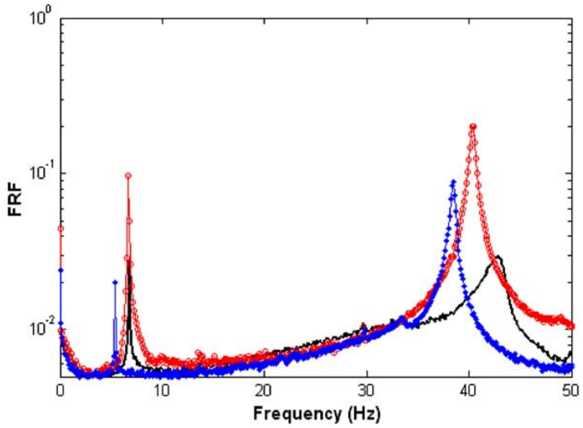

Fig. 4. First two natural frequencies of the experimental structure: ——, plate added; —○—, original structure; —•—, tip mass added.

values, which results in the adaptive prediction model. Since the CARIMA model integrates the plant and the disturbance models, a relatively larger plant order ($n = 9$) is used here to capture plant dynamics adequately. The predicted (tip) acceleration was used to calculate the performance index and to determine the best control signal that minimizes the performance index.

Figs. 5–7 show the uncontrolled and controlled responses of the plant for several excitations generated by the shaker. The excitation voltage sent to the shaker amplifier and the resulting tip accelerations are presented. Since the reduction of vibrations in the r.m.s sense has a very significant effect on the fatigue life of a structure, the r.m.s. reductions were computed for a 10 s time period. The figures show responses for smaller durations for the clarity of presentation. For first and second mode sine wave excitations, r.m.s. reductions of 73% and 87%, respectively, were achieved. Even for a band-limited white noise (0–50 Hz) disturbance (Fig. 7), a large r.m.s. reduction of 61% was observed.

To analyze the response in the frequency domain, a combination of first and second mode frequencies was used. The experiment was repeated five times for both uncontrolled and controlled cases to obtain the average values and the uncertainty in the results. The frequency response (Fig. 8) shows an average vibration reductions of 13 and 19 dB at the first and second natural frequencies, respectively. The maximum uncertainty of ± 1.3 dB was observed in these measurements.

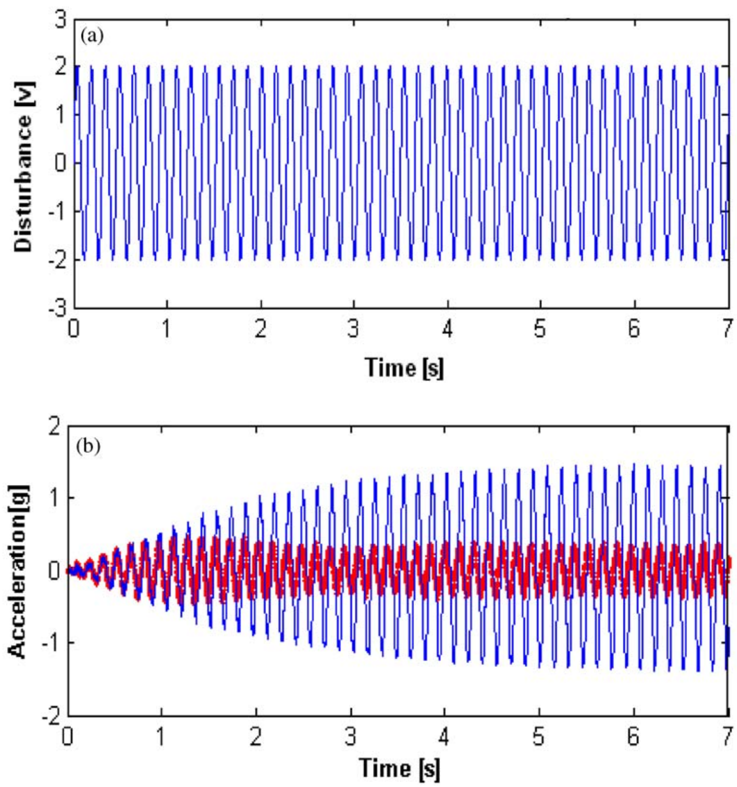

Fig. 5. (a) First mode sine wave disturbance and (b) response to excitation at first natural frequency: ——, uncontrolled; —•—, controlled.

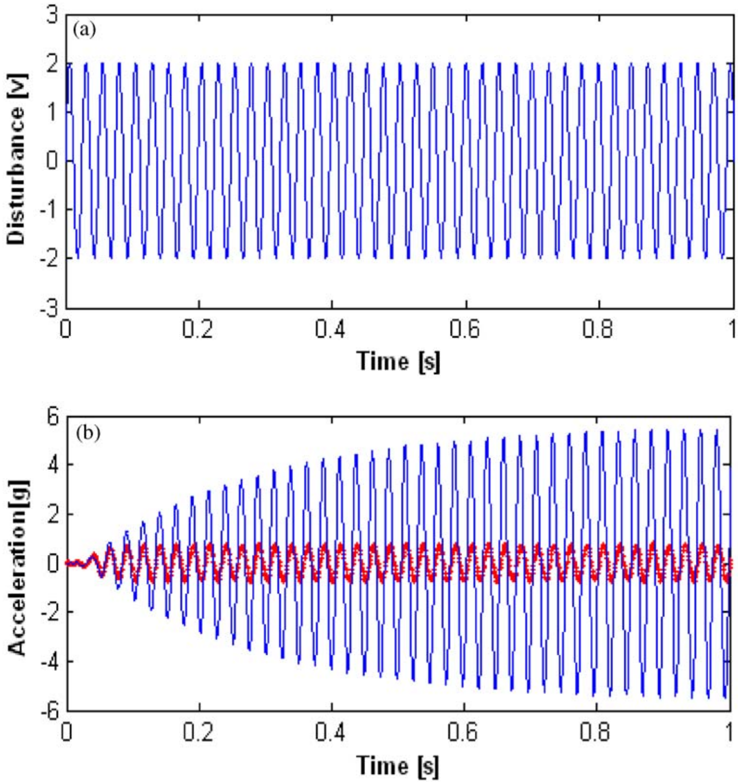

Fig. 6. (a) Second mode sine wave disturbance and (b) response to excitation at second natural frequency: ——, uncontrolled; —•—, controlled.

In many practical situations, the system dynamics or external excitations may change with time for various reasons. A robust controller is therefore desired to maintain satisfactory performance with perturbations in the system. To clearly show the robustness of the AGPC, the excitation frequency was changed from first mode to second mode after 7 second (Fig. 9) and from second mode to first mode in about 3 s (Fig. 10). The figures show that the controller adjusts its parameters quickly and continues to perform very well even after such large changes in the excitation frequency.

To test the experimental performance of adaptiveness, modifications to the original structure (Fig. 2(a)) are used. One modification is adding a plate to the original structure, which basically increases the stiffness of the structure (Fig. 2(b)). The other modification is adding a mass near the tip (Fig. 2(c)), which decreases the natural frequencies. The controller was tested for the modified structures using sine wave disturbances at the first two natural frequencies (Figs. 11–14). For the plate-added case, first and second mode r.m.s. reductions of 72% and 79%, respectively, were achieved. The r.m.s. vibrations at the first and second natural frequencies decreased by 68% and 80%, respectively, for the tip mass added case. These vibration reductions are similar to those for the original structure indicating that the developed controller is highly adaptive.

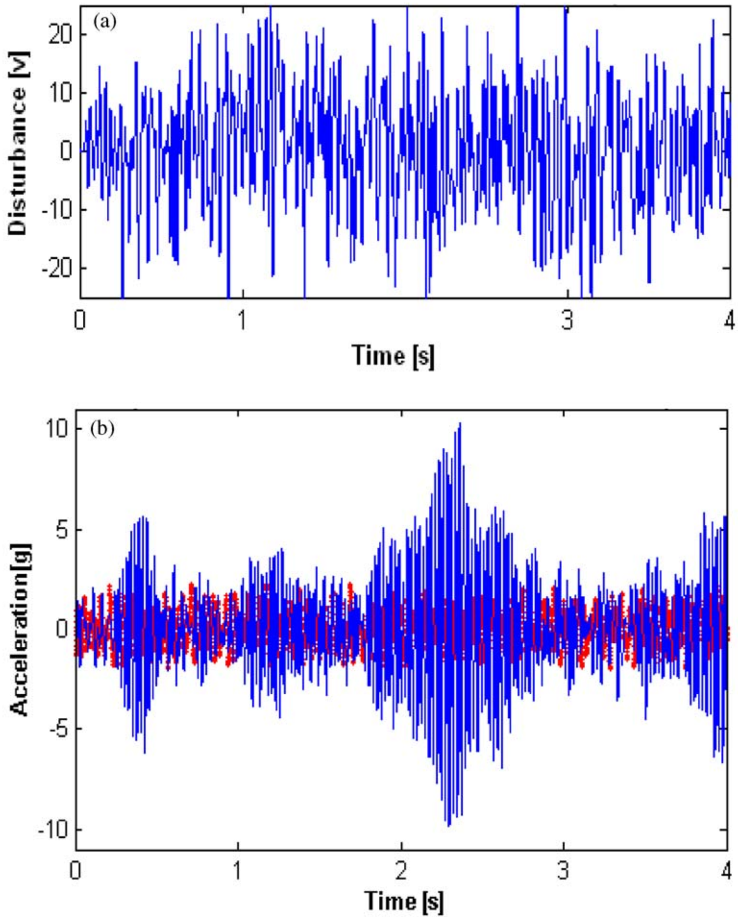

Fig. 7. (a) Band-limited white noise excitation (0–50 Hz) and (b) response to band-limited white noise excitation: ——, uncontrolled; —●—, controlled.

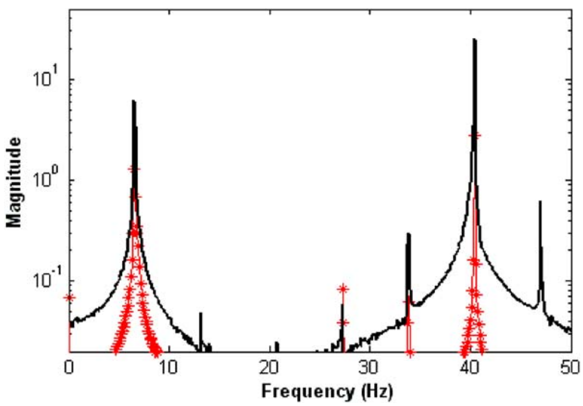

Fig. 8. Response to excitation at first and second natural frequencies: ——, uncontrolled; —★—, controlled.

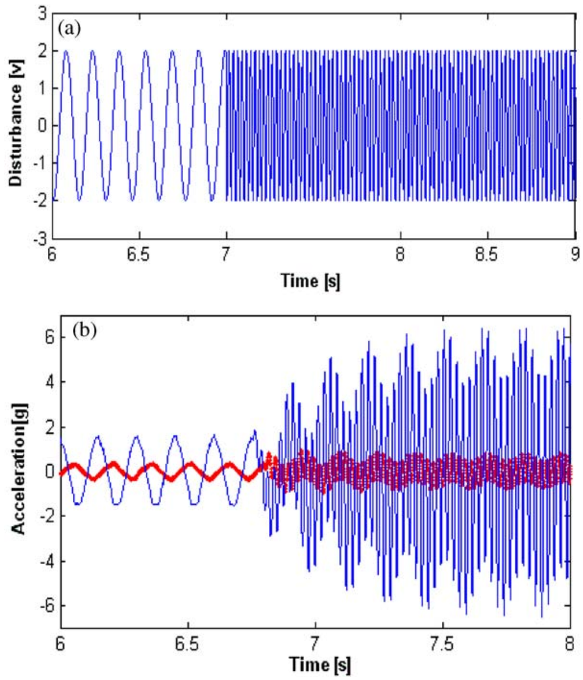

Fig. 9. (a) Excitation change from first to second natural frequency and (b) response to excitation change from first to second natural frequency: ——, uncontrolled; —•—, controlled.

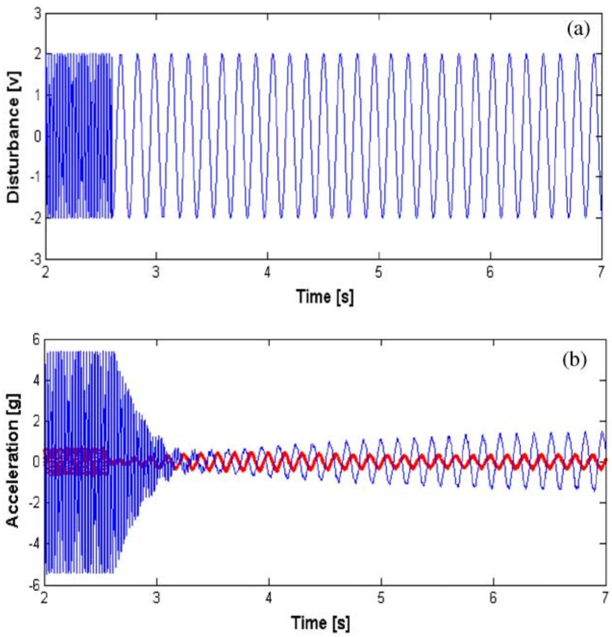

Fig. 10. (a) Excitation change from second to first natural frequency and (b) response to excitation change from second to first natural frequency: ——, uncontrolled; —•—, controlled.

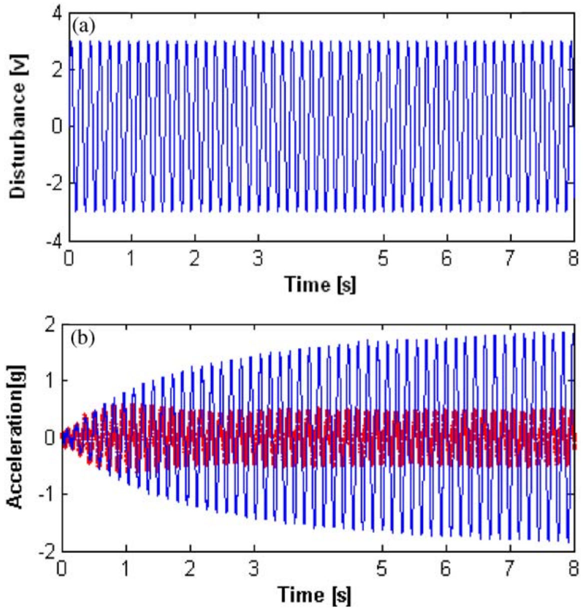

Fig. 11. (a) First mode sine wave disturbance and (b) response to excitation at first natural frequency (plate added structure): ——, uncontrolled; —•—, controlled.

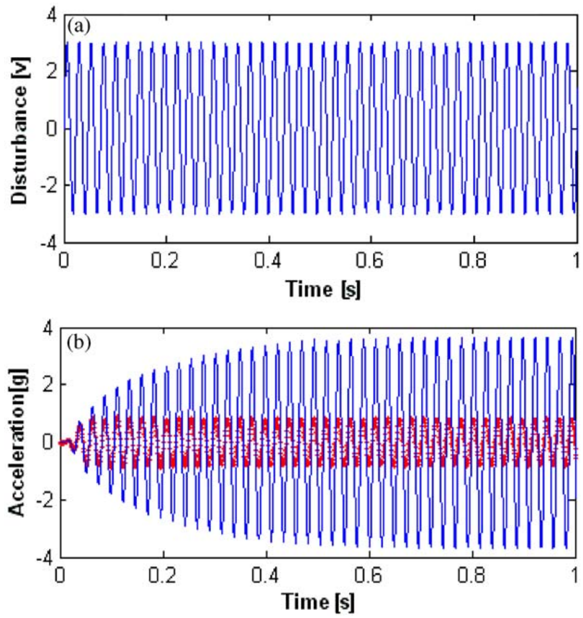

Fig. 12. (a) Second mode sine wave disturbance and (b) response to excitation at second natural frequency (plate added structure): ——, uncontrolled; —•—, controlled.

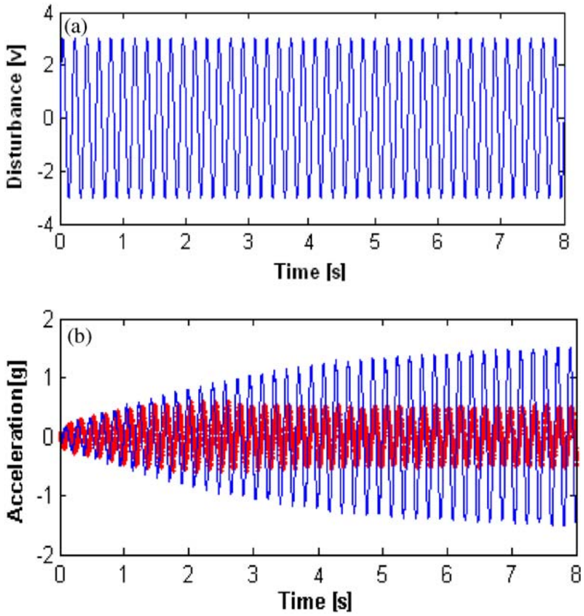

Fig. 13. (a) First mode sine wave disturbance and (b) response to excitation at first natural frequency (tip mass added structure): ——, uncontrolled; —•—, controlled.

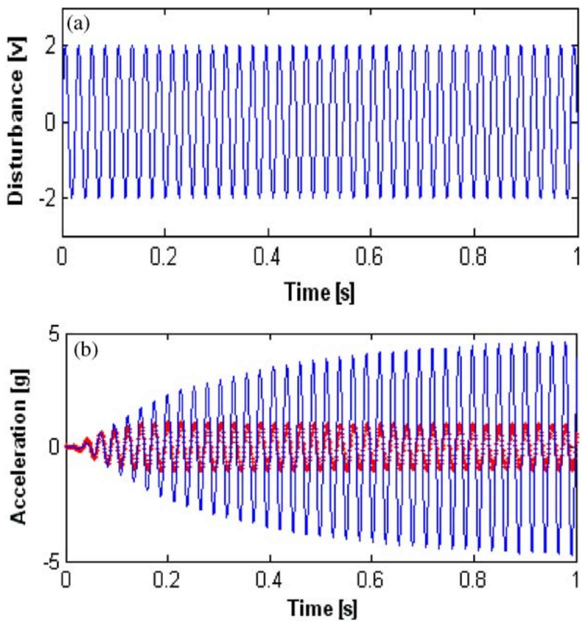

Fig. 14. (a) Second mode sine wave disturbance and (b) response to excitation at second natural frequency (tip mass added structure): ——, uncontrolled; —•—, controlled.

4. Conclusions

This paper presents an experimental evaluation of AGPC for vibration suppression of smart structures. The controller development follows the generalized predictive control methodology with the plant represented by a controlled auto-regressive integrated moving average model. The one-step-ahead plant model is obtained online using augmented UD identification in real time. This efficient and robust technique is capable of coping with system uncertainty and time variation. The performance index comprises a weighted sum of quadratic functions representing predicted future errors and control signal increments.

Experimental evaluation of the control system is performed using a cantilevered plate with two surface bonded piezoelectric patch actuators at the root and an accelerometer (sensor) at the tip. The r.m.s. vibration reductions range from approximately 60% to 90% for white noise and sine wave (at the first and second natural frequencies) disturbances. In the frequency domain, 13–19 dB reductions are achieved (with a maximum uncertainty of $\pm 1.3\,\mathrm{dB}$) for sine wave disturbances. A similar performance is obtained with the structure modified by attaching another plate or a tip mass. The controller continues to perform well when the excitation frequency is changed from first mode to second mode and vice versa. These results demonstrate very good closed-loop performance and adaptiveness of the controller.

References

[1] H.S. Tzou, G.L. Anderson (Eds.), *Intelligent Structural Systems*, Kluwer Academic Publishers, Dordrecht, The Netherlands, 1992.
[2] R. Isermann, K.H. Lachmann, D. Matko, *Adaptive Control Systems,* Prentice-Hall International, UK, 1992.
[3] G.A. Dumont, M. Huzmezan, Concepts, methods, and techniques in adaptive control, *Proceedings of the American Control Conference*, Anchorage, AK, May 8–10, 2002, pp. 1137–1150.
[4] D.W. Clarke, C. Mohtadi, P.S. Tuffs, Generalized predictive control—Part I the basic algorithm, *Automatica* 23 (2) (1987) 137–148.
[5] D.W. Clarke, C. Mohtadi, P.S. Tuffs, Generalized predictive control—Part II extensions and interpretations, *Automatica* 23 (2) (1987) 149–160.
[6] R.G. Kvaternik, J.-N. Juang, R.L. Bennett, Exploratory Studies in Generalized Predictive Control for Active Aeroelastic Control for Tiltrotor Aircraft, NASA/TM-2000-210552, NASA Langley Research Center, October 2000.
[7] S. Niu, D.G. Fisher, D. Xiao, An augmented UD identification algorithm, *International Journal of Control* 56 (1) (1992) 193–211.
[8] M.E. Salgado, G.C. Goodwin, R.H. Middleton, Modified least squares algorithm incorporating exponential resetting and forgetting, *International Journal of Control* 47 (2) (1988) 477–491.
[9] G.J. Bierman, *Factorization Methods for Discrete Sequential Estimation*, Academic Press, New York, 1977.
[10] D.W. Clarke, Adaptive predictive control, *Annual Reviews in Control* 20 (1996) 83–94.
[11] V.M. Maniar, S.L. Shah, D.G. Fisher, R.K. Mutha, Multivariable constrained adaptive GPC: theory and experimental evaluation, *International Journal of Adaptive Control and Signal Processing* 11 (4) (1997) 343–365.
[12] S. Niu, D. Xiao, D.G. Fisher, A recursive algorithm for simultaneous identification of model order and parameters, *IEEE Transactions on Acoustics, Speech and Signal Processing* 38 (5) (1990) 884–886.
[13] J.-N. Juang, K.W. Eure, Predictive Feedback and Feedforward Control for Systems with Unknown Disturbances, NASA TM-1998-208744, December 1998.
[14] A. Chattopadhyay, C.E. Seeley, R. Jha, Aeroelastic tailoring using piezoelectric actuation and hybrid optimization, *Smart Materials and Structures* 8 (1999) 83–91.